



1 Multi-hazards in Scandinavia: Impacts and risks from compound 2 heatwaves, droughts and wildfires

3 Gwendoline Ducros³, Timothy Tiggeloven¹, Lin Ma², Anne Sophie Daloz², Nina Schuhen², and Marleen C. de Ruiter¹

4 ¹ *Institute for Environmental Studies, Vrije Universiteit Amsterdam, 1081 HV Amsterdam, The Netherlands*

5 ² *CICERO Center for International Climate Research, Oslo 0318, Norway*

6 ³ *independent researcher (formerly at: Institute for Environmental Studies, Vrije Universiteit Amsterdam, 1081 HV Amsterdam,*
7 *The Netherlands)*

8 *Correspondence to:* Gwendoline Ducros (gwendolineducros@gmail.com)

9 10 **Abstract.**

11 In the summer of 2018, large parts of Scandinavia faced record-breaking heat and drought, leading to increased
12 mortality, agricultural water shortages, hydropower deficits, and higher energy prices. The 2018 heatwave coupled
13 with droughts leading to wildfires are described as multi-hazard events, defined as compounding, cascading or
14 consecutive events. Climate change is driving an increase in heat-related events and, subsequently, shows the necessity
15 to prepare for such hazards, and to assess suitable adaptation measures. To better understand the interplay of multi-
16 hazard risk of heatwaves, droughts and wildfires in a multi-sectoral context and to improve disaster risk management
17 in a multi-hazard setting, we assess the occurrence of these hazards using a spatial analysis of compound heatwave,
18 drought and wildfire events in Scandinavia. To assess their potential direct and indirect economic impacts we use the
19 global Computable General Equilibrium (CGE) model GRACE (Global Responses to Anthropogenic Changes in the
20 Environment) and the 2018 heatwave-drought period as a baseline to map multi-hazard risk. We find that multi-hazard
21 events are pronounced in the summer months in Scandinavia and the 2018 multi-hazard events did not occur in
22 isolation. The 2018 multi-hazard events led to a 0.08% GDP drop in Scandinavia, with forestry experiencing a 3.04%
23 decline, affecting agriculture, electricity, and forestry exports, which dropped by 29.39%, impacting Europe's trade
24 balance. This research shows the importance of ripple effects of multi-hazard, and that forest management and
25 adaptation measures are vital to reducing the risks of heat-related multi-hazards in vulnerable areas.



26 1 Introduction

27 In the summer of 2018, in particular over the period May-August, large parts of Scandinavia experienced record-
28 breaking temperatures and extreme drought (Bakke et al., 2020). These climate conditions were linked to severe
29 repercussions on human health and the ecosystem, leading to an increased mortality rate during that period (Åström
30 et al., 2019), water shortages that impacted agricultural areas (Buras et al., 2020), as well as hydropower energy deficit
31 and an increase in energy prices (Norwegian Water Resources and Energy Directorate, 2018). The temperature
32 anomalies experienced during the months of May to July were found to be enhanced by human-induced climate change
33 (Wilcke et al., 2020), amongst other factors (Kueh et Lin, 2020).

34 Heat-related events are expected to increase in frequency, severity, and intensity in the future as a result of
35 anthropogenic climate change (IPCC, 2021). Anthropogenic climate change is also predicted to intensify fire and
36 drought frequency in boreal ecosystems (Girardin et al., 2010; IPCC, 2021) with winter warming expected to increase
37 in boreal forests due to decreasing snow cover and albedo (IPCC, 2021). Spatial patterns of snow cover already show
38 a declining trend in Scandinavia (Brown and Mote, 2009) and the northern area of Scandinavia even sees a projected
39 increase in temperature twice as much as average global warming in winter (Christensen et al., 2022).

40 The 2018 heatwave coupled with droughts leading to wildfires events are described as multi-hazard events
41 which can occur as compound events if they happen simultaneously, or consecutive events if they occur one after the
42 other (Sutanto et al., 2020; Zscheischler et al., 2017; De Ruiter et al., 2020). This study will focus on compound events,
43 defined here as two or more extreme events occurring at the same time (same day and same region), following the
44 definition from Zscheischler et al., 2017. Specific compound events can be explained by feedback mechanisms, where
45 interactions between climate processes can lead to a positive feedback loop and exacerbate the effects of multiple
46 hazards (IPCC 2012; Zscheischler et al., 2017; Raymond et al., 2020; AghaKouchak et al., 2020). Tilloy et al. (2019)
47 provided a thorough overview of different quantification methods used in the literature for multi-hazard interactions,
48 classifying approaches in stochastic, empirical, and mechanistic methods. In recent years, compound studies have
49 increasingly made use of multivariate-statistical modeling techniques (Couasnon et al. 2020; Mazdiyasi &
50 AghaKouchak 2015; Paprotny et al. 2020; Moftakhari et al. 2019; Wahl et al. 2015).

51 The projected increase in heat-related events shows the necessity to prepare for such hazards, and to assess
52 suitable adaptation measures. Although the probability of compound events is predicted to increase with the rise in
53 global temperature (IPCC, 2021), mitigation and adaptation measures for multi-hazard compound events have only
54 recently begun to be addressed. Frameworks such as the Sendai Framework for Disaster Risk Reduction (SFDRR)
55 have been adopted by the United Nations with the goal of decreasing disaster risk and increasing resilience,
56 underlining the importance of looking at multi-hazard risk when implementing Disaster Risk Reduction (DRR)
57 measures (UNDRR, 2015). Several studies have emphasized that adaptation strategies and policies are more effective
58 when taking into account multiple stressors (Scolobig et al., 2017; IPCC 2012; de Ruiter et al. 2021; Schipper, 2020;
59 Berrang-Ford et al., 2021). Research has found that certain adaptation measures put into place for a specific hazard
60 might negatively impact adaptation measures against another hazard (de Ruiter et al., 2021), such as the potential of
61 flood DRR measures to increase the risk of droughts and vice versa (Ward et al., 2020). Accounting for multi-hazards
62 in DRR measures decreases the probability that an adaptation measure designed for a singular hazard increases the
63 risk for another (Zscheischler et al., 2017; Raymond et al., 2020; AghaKouchak et al., 2020).

64 Moreover, heat-related events can have severe direct and indirect economic impacts on sectors such as
65 agricultural or energy production. For example, annual economic losses caused by droughts are currently estimated at
66 around 9€ billion for the EU and the UK, with agriculture amounting to 30-60% of losses and the energy sector to 22-
67 48% (European Commission: Joint Research Centre, 2020). Nearing the end of the 21st century, these losses are
68 estimated between 25 and 45€ billion, depending on the climate scenario, and with no adaptations put into place
69 (European Commission: Joint Research Centre, 2020). Additionally, socio-economic impacts of compound events
70 may surpass those predicted by examining each driver individually (Matano et al., 2021). With this perspective it is
71 thus crucial to include multi-hazard risk when analyzing economic impacts of heat-related events.

72 To better understand the interplay of multi-hazard risk of heatwaves, droughts and wildfires in a multi-
73 sectoral context and to improve disaster risk management in a multi-hazard setting, we assess the occurrence of these

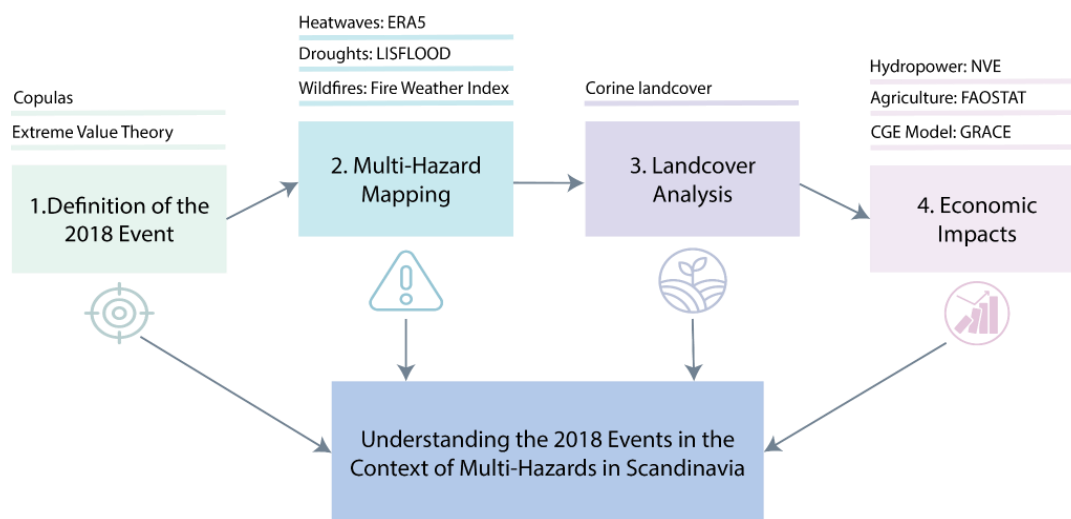


74 hazards using a spatial analysis of compound drought, wildfire, and heatwave events from 2000 to 2018 in Scandinavia
75 (here Finland, Norway and Sweden). To assess their potential direct and indirect economic impacts we use the global
76 Computable general equilibrium (CGE) model GRACE (Global Responses to Anthropogenic Changes in the
77 Environment) and the 2018 heatwave-drought period as a baseline. CGE models or partial equilibrium models are
78 commonly used to evaluate the economic impacts of changes in agriculture and food production (Ntombela et al.,
79 2017, Manuel et al., 2021; Solomon et al., 2021).

81 2 Data & Methods

82 To assess and better understand the multi-hazard risk and impacts in Scandinavia during the 2018 multi-hazard event,
83 we first identify past trends and patterns, as these provide essential context for evaluating the event's economic
84 impacts. Our methodology includes the following steps: First, we define historical multi-hazard events using the
85 ERA5 global climate and weather reanalysis (Hersbach et al., 2023) and a copula function describing the correlation
86 structure between key variables (section 2.1). The second part (section 2.2) focuses on mapping multi-hazard risk, for
87 which we will map different combinations of compound heatwave, droughts and wildfires events over the period
88 2000-2018, and, from this, map the 90th percentile of the compound multi-hazards. Section 2.3 maps out Scandinavian
89 land cover using data from the Copernicus Land Monitoring Service, and uses the multi-hazard risk maps and land
90 cover maps to map the main land cover types at highest risk of multi-hazards. Lastly, section 2.4 will cover the
91 economic impacts of the 2018 multi-hazard event using GRACE. Together, these methods increase understanding of
92 Scandinavian multi-hazard events in summer.

93



94

95 **Figure 1.** Flowchart describing the methodology and data used in the study

96 2.1 Definition of the 2018 multi-hazard event

97 We investigate the optimal objective definition of the heat wave and drought compound event that occurred across
98 Europe in spring and summer 2018. As the area of interest is restricted to Northern European countries - namely
99 Finland, Norway and Sweden - the domain is restricted to land masses of these three countries (below 67° N). The
100 analysis is based on data from the ERA5 reanalysis for March to September, in the time period 1979-2023 on daily
101 temporal resolution.

102 To obtain the event definition, we proceed in three steps, first estimating climatological distributions for each
103 variable (daily maximum surface temperature and total precipitation) from the full data set, then connecting the



104 univariate distributions with a copula to get a multivariate joint distribution, and finally look for the time period with
105 the smallest event probability, based on the maxime that the extreme nature of such an event is best characterized by
106 minimizing its rarity (Schuhen et al. (2024); see Cattiaux and Ribes (2018) for more details on the univariate
107 procedure).

108 To estimate the marginal distributions, we collect, for each day and year in March-September of the data set,
109 the maximum (for temperature) or minimum (for precipitation) value over a temporal neighborhood of 7 days on
110 either side. This is to ensure a more robust and smoother estimation. For a large range of potential event dates and
111 durations, these values are then averaged over the respective time period and area, before a standard probability
112 distribution is fitted to each scale (Gaussian distributions for temperature and generalized extreme value distributions
113 for precipitation).

114 To combine the two marginal distributions into a bivariate distribution, we use a copula, which is a
115 multivariate cumulative distribution function describing the correlation structure between the variables, independent
116 of the marginal distributions. In this case, we found that the symmetrical Frank copula best represents the relationship
117 between temperature and precipitation. Finally, we compute from this distribution the joint probability that
118 temperature would exceed the 2018 value and precipitation would be lower than the 2018 values. This procedure is
119 repeated for the whole range of potential temporal scales of different dates and durations between May and September
120 2018, and we finally find the minimum in the set of probabilities, which is associated with the objective event
121 definition.

122 **2.2 Multi-hazard mapping of historical events**

123 This study builds on and uses datasets previously generated by Sutanto et al., (2020) containing the required heatwave,
124 drought and wildfire data that have been used for this analysis. Sutanto et al. (2020) analyzed drought, heatwave and
125 wildfire events occurring in the months of June, July and August (JJA) from 1990 to 2018 at the pan-European scale.
126 Weather data for heat waves was drawn from ERA5, soil moisture drought simulated through the LISFLOOD model,
127 and wildfire estimated with the Fire Weather Index. They analyzed the frequency and spatial distribution of
128 occurrences of these hazards, and created daily binary maps (0 indicating no risk, and 1 indicating a risk). This resulted
129 in three datasets of 2886 maps each (one map for each summer day of JJA over the period 1990-2018).

130 The Copernicus Land Monitoring Service inventories Scandinavian land cover starting in the year 2000. For
131 consistency with the Corine Land Cover (CLC) datasets that are used in part 2.2, the study period for this research is
132 thus 2000-2018. The hazard datasets were analyzed to create four compound hazards maps of the following
133 combinations: drought and wildfire (DF), heatwave and wildfire (HF), heatwave and drought (HD), and drought,
134 heatwave and wildfire (DHF) over the period 2000-2018. First, we developed maps indicating the percent of summer
135 days at risk of the hazard combinations by adding for each hazard combination, the individual hazard maps together,
136 and dividing by the amount of summer days over the period 1990-2018. To cover the study period, a subset was
137 created from the period 1990-2018 to cover the period 2000-2018, for each hazard combination, and divided by the
138 amount of summer days during the 2000-2018 period, which corresponds to 1656 summer days (see formula below).
139 The resulting maps indicated the percent of summer days at risk of each hazard combination.

140

141 *Percent of days with an event*

$$142 = (\text{number of days with an event} / \text{total number of summer days}) * 100$$

143

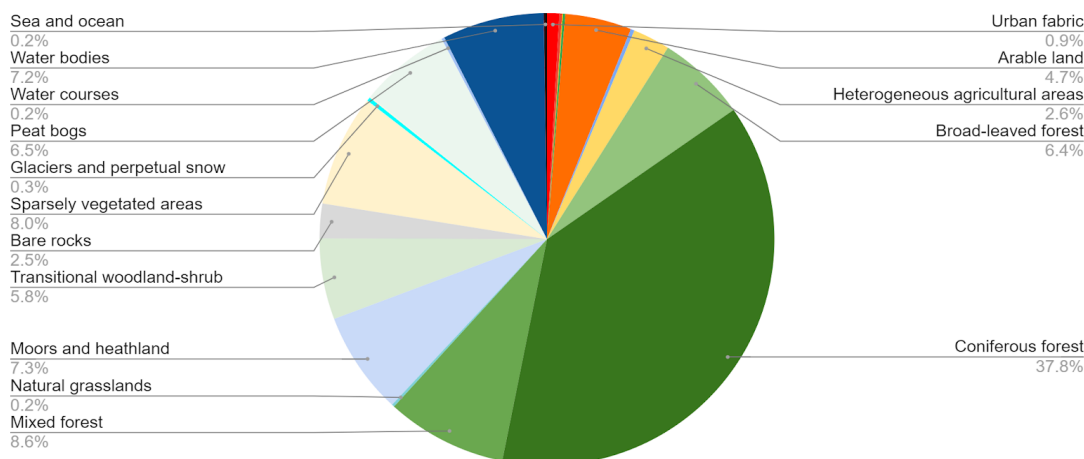
144 To simplify the compound hazard maps, we calculated the 90th percentile of percent of days of each
145 compound hazard map to produce binary compound risk maps, with 0 corresponding to no risk of a compound hazard
146 combination, and 1 to a risk of a compound hazard combination. The above-mentioned percentile was chosen
147 following Sutanto et al.'s (2020) calculations.

148 Lastly, compound hazard maps for the study area, Scandinavia, were generated by clipping the binary 90th
149 percentile compound hazard maps with the region of Scandinavia, from Nuts-1 region maps provided by Eurostat, and
150 extracting only the Scandinavian region.



151 **2.3 Analysis of land cover type in areas at high risk of multi-hazard compound events**

152 Next, we generated a land cover map of Scandinavia using data from the CORINE Land Cover (CLC) inventory
153 provided by the Copernicus Land Monitoring Service. The raster files over the period 2000-2018 and CLC legend
154 were used to classify land cover types, as seen in annex 1. Figure 4 below shows the percentage share of land cover
155 in Scandinavia for the year 2018.



156
157 **Figure 2.** Percent of total land per land cover type in 2018.

158
159 As seen in Fig. 2, coniferous forests cover the majority of Scandinavia, accounting for 37.8% of the total
160 surface area and mostly in Sweden and Finland where land cover is largely dominated by coniferous forests, as
161 expected due to their economic reliance on the timber industry. Mixed forests and sparsely vegetated areas are the
162 next most extensive land cover, accounting for 8.6% and 8.0% of the total surface area, respectively. In contrast to
163 Sweden and Finland, Norway has a very high proportion of this sparsely vegetated area, and broad-leaved forests
164 (6.4% of Scandinavia) are also mainly found in Norway and along the Norwegian-Swedish border. Arable land and
165 heterogeneous agricultural areas account for respectively 4.7% and 2.6% of total land cover. Urban fabric only
166 accounts for 0.9% of the total surface area in the region whilst the vast majority of arable land is located in Southern
167 Sweden and Finland.

168
169 In order to produce the main land cover types affected by the studied compound hazard combinations, the
170 multi-hazard maps of Scandinavia from section 2.2.2 were overlaid with the land cover map of Scandinavia generated
171 in 2.2.3, using the multi-hazard maps as references for resolution. Subsequently, we derived the amount of land
172 affected by each hazard combination per land cover type with spatial analysis.

173 **2.4 Assessing economic impacts of multi-hazard risk in Scandinavia**

174 We define here direct economic loss as “monetary value of total or partial destruction of physical assets existing in
175 the affected area” and indirect economic loss as “a decline in economic value added as a consequence of direct
176 economic loss and/or human and environmental impacts” (UNDRR, 2017).

177 **2.4.1 Economic Model**

178 To assess the economic impacts of multi-hazard risk, we employ a multi-region, multi-sector computable general
179 equilibrium (CGE) model, Global Responses to Anthropogenic Changes in the Environment (GRACE) (Aaheim et al.



180 2018). The GRACE model follows the standard assumptions in most CGE models, including assumptions for
181 producers, Regional Households (RH) and the market dynamics. In this paper, the parameters in the GRACE model
182 are calibrated using the global social accounting data in 2014 in the Global Trade Analysis Project (GTAP) database
183 version 10 (Aguilar et al., 2019). In order to address the impacts of the 2018 Scandinavia multi-hazards within the
184 European area, we divided the global region into 33 European countries¹ and the rest of the world. Each country and
185 region is further divided into 11 sectors: agriculture, forestry, fishery, manufacturing, services, transportation, crude
186 oil, coal, gas, refinery, and electricity. The static version of the GRACE model is solved at the country-sectoral level
187 on an annual basis. With significant advantages in the GRACE model due to the multi-sector and multi-region setup,
188 the model is able to provide a comprehensive analysis on how the sectoral-specific shocks, such as those caused by
189 the natural hazards, transfer to other sectors and parts of the economy through the value chain effects. Meanwhile, it
190 also reveals how the country-specific effects due to hazards spill over to other regions through the trade, which makes
191 it particularly useful for assessing the broader economic consequence of multi-hazard events.

192 2.4.2 Sectoral context in Scandinavia

193 As discussed in the previous section, the direct impacts of the 2018 multi-hazards are mainly focused on agriculture,
194 forestry, and energy. Therefore, in this research, we employ various methods to assess the direct physical impact of
195 2018 natural hazards on the production of these targeted sectors, which is the input of the macroeconomic model for
196 evaluating the indirect impacts.

197 2.4.3 Estimating sectoral heat-induced impact

198 For estimating the direct sectoral impact functions, we employed the dataset on the annual production of agriculture
199 goods in the Scandinavia region for the period 1961 – 2020 from Food and Agriculture Organization Corporate
200 Statistical Database (FAOSTAT) (2023). This study approximates total hydroelectricity production using aggregate
201 reservoir storage volume, as recommended by Norwegian Water Resources and Energy Directorate (NVE) (2019).
202 Due to the limited availability of daily hydroelectricity production data, we use the weekly reservoir level for Norway
203 for the period 1995–2022, collected from NVE (2024), as the representative of the region. This estimation employs
204 climate data extracted from Lund et al. (2023)

205

206 We employ econometric models to assess the direct physical impacts of extreme weather events on agriculture and
207 energy production following Aaheim et al. (2012). Initially, we estimate the relationship between climatic variables
208 and sector-specific outputs, utilizing the observational data detailed in Section 2.3.2. For this analysis, a log-level
209 model is employed. The model formulation is as follows:

$$210 \log(Q_t^i) = \alpha_i + \beta_i X_t^{climate} + \pi_i X_t^{control},$$

211 where Q_t^i represents the production of sector i . $X_t^{climate}$ denotes the vector of climate variables, which includes the
212 average weekly temperature, precipitation and their interaction terms. It includes $[\Delta T, \Delta P, T \times \Delta T, P \times$
213 $\Delta P, \Delta T^2, \Delta P^2, T \times P]$. $X_t^{control}$ denotes the vector of control variables. When estimating the impact function for the
214 energy sector, $X_t^{control}$ comprises month, year, and country dummy variables. When estimating the impact function
215 for the agriculture and forestry sectors, $X_t^{control}$ includes year and country dummy variables.

216 To estimate the impact functions, we utilize the forward selection method. This stepwise regression approach
217 identifies the most significant variables for inclusion in our regression model. We selected the regression model that
218 best fits the empirical data, as indicated by the highest R-squared value. Table 1 reports the estimated percentage
219 change of production of agriculture and electricity products, β_i , in the climate-impact functions. Only estimates that
220 are statistically significant at confidence level $\alpha=0.05$ are reported and employed in the GRACE model. All values

¹ The European countries are Austria, Belgium, Bulgaria, Croatia, Cyprus, Czech Republic, Denmark, Estonia, Finland, France, Germany, Greece, Hungary, Ireland, Italy, Latvia, Lithuania, Luxembourg, Malta, Netherlands, Poland, Portugal, Romania, Slovakia, Slovenia, Spain, Sweden, United Kingdom, Switzerland, Norway, Albania, Belarus, Ukraine.



221 have been adjusted to annualized measures for consistency used for the assessment of economic impacts in the
 222 GRACE. These results update the previous estimation outcome in Aaheim et al. (2012) for the Scandinavia region,
 223 and the magnitude of unit impacts remains consistent.

224 **Table 1.** Estimated percentage change of sectoral production (annualized)

SECTOR	ΔT	ΔP	$T \times \Delta T$	ΔP^2	ΔT^2
Agriculture	0.0045	0.0123	-0.0012	0.0007	0.0014
Electricity	0.0076	0.0035			-0.0007

225

226 Next, we assess the direct physical impact on agricultural and energy production resulting from extreme weather
 227 events in 2018. To do this, we calculate the 95th percentile of climate variable deviations from their climatological
 228 norms for the year 2018. Our analysis reveals a significant deviation, indicating a temperature increase of 5.50°C and
 229 a precipitation decrease of 170 mm.

230

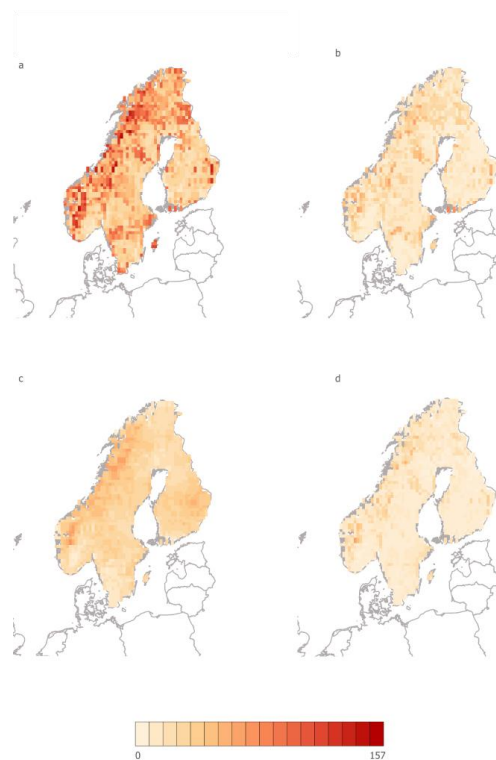
231 Finally, we assess the impact on the forestry sector. We utilized the assessment detailed in Section 3.2, and
 232 computed 6% of the forest area was affected by the multi-hazard event. We use the share of the area impacted by the
 233 drought-wildfire-heat events as a proxy to assess the effect on the production of forestry. However, this approach
 234 oversimplifies by not accounting for the heterogeneity of plant density and yield rates across different tree species.
 235 This could potentially lead to inaccuracies in our measurements, which could be extended for further research.

236

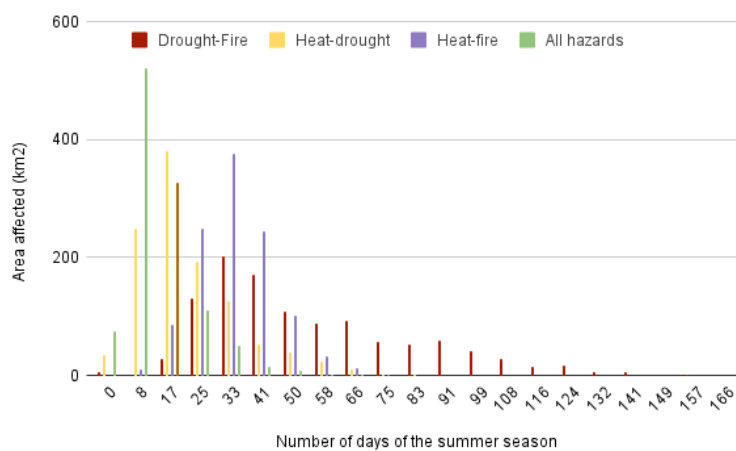
237 3 Results

238 3.1 Spatial distribution of compound hazard events in Scandinavia

239 High risk drought-wildfire events occur twice as often as heat-wildfire, and heat-drought events, with occurrences up
 240 to 166 days of the summer seasons between 2000-2018, as seen on Fig. 3 below. The majority of areas across
 241 Scandinavia have low risk of compound combination hazards (from 0 to 41 days of the summer seasons). Although
 242 the risk is currently very low for most areas, droughts and wildfires in boreal ecosystems are expected to escalate with
 243 rising global temperatures (IPCC, 2021).



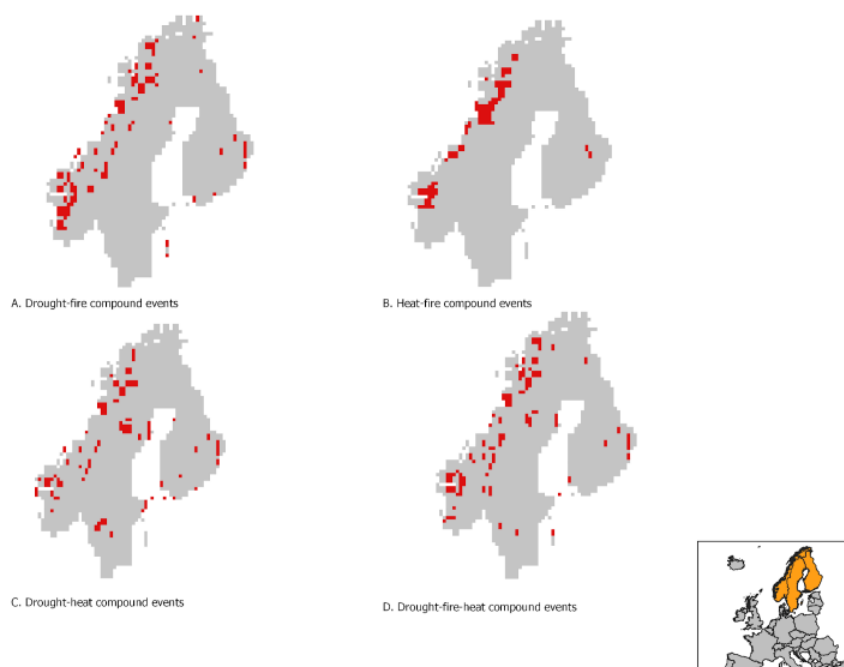
244
245 **Figure 3** Spatial distribution of compound heat-related events, in number of summer days, over the period 2000-2018
246 (a. Drought-wildfire, b. Heat-drought, c. Heat-wildfire, d. Drought-wildfire-heat).
247



248
249 **Figure 4.** Amount of land (in km²) affected by the compound hazard combinations, in number of days, over the period
250 2000-2018.



251 We located hotspots by calculating the 90th percentile of percent of days, which can be seen in Fig. 5 below. Drought
252 and wildfire compound events are mainly located along the Norwegian coast (panel A). Heat and wildfire events
253 are also mainly located along the Norwegian coast, and along the Norwegian-Swedish northern border (panel B). Heat
254 and drought events are located along the Norwegian coast as well, though there are noticeably more hotspots more in-
255 land (panel C). There is a lot of overlap in areas where conditions are conducive to multi-hazard heat-related events.
256 These areas are at risk of all manner of compound events whereas most in-land regions are not at risk of any compound
257 events.



258

259

260 **Figure 5.** Spatial distribution of compound multi-hazard risk in Scandinavia. Figure shows the 90th percentile of
261 compound events over the JJA period of 2000-2018; (a. Drought-wildfire, b. Heat-wildfire, c. Drought-heat, d.
262 Drought-wildfire-heat).

263

264 3.2 Land cover of 90th percentile of percent of days

265 All hazard-combinations affect significantly moors and sparsely vegetated areas (Table 2). The moors are mainly
266 located along the northern Norwegian-Swedish border and south-western region of Norway (Fig. 6 below). Broad-
267 leaved forests are at high risk of all compound hazard combinations, and are found along the northern Norwegian-
268 Swedish border and south-western region of Norway. Coniferous forests are at quite low risk of heat-wildfire
269 compound events (only 5.5% of total affected area), but are at significantly higher risk of heat-drought compound
270 events (18.2% of total affected area). These coniferous forests are located in the south-western region of Norway,
271 along the northern Norwegian-Swedish border, central Sweden and in the south-eastern region of Finland. Water
272 bodies are at higher risk of heat-drought events than the other compound combination events. These are mainly found
273 in south-western Sweden (Fig. 16). Bare rocks are at high risk of all combinations of compound events.



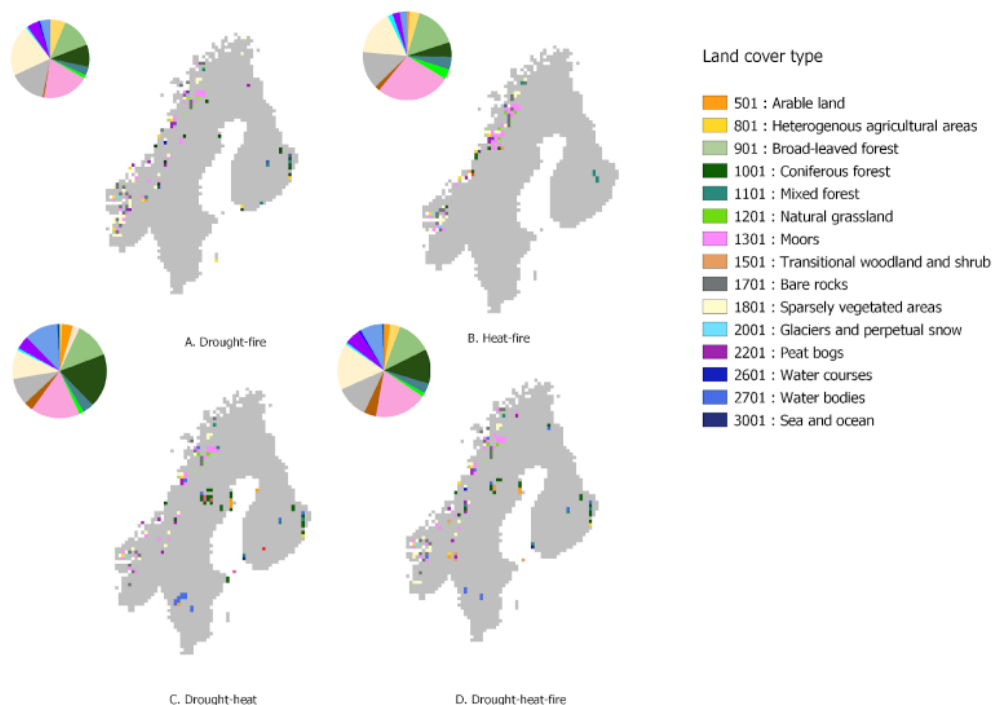
274 **Table 2.** Main land cover types affected by heatwave, droughts and wildfires compound events combinations, by
275 percent of the total area affected.
276

	Bare rocks	Broad-leaved forests	Coniferous forests	Sparsely vegetated areas	Moors and heathland	Water bodies
Drought-wildfire	14.9	12.8	9.2	21.3	19.1	4.3
Heat-wildfire	13.6	15.5	5.5	16.4	27.3	2.7
Heat-drought	9.2	12.3	18.5	16.2	16.9	11.5
Drought-wildfire-heat	11.3	12.0	12.0	16.2	18.3	7.7

277



278



279

280 **Figure 6.** Land cover type and land cover share of areas at high risk of compound events; (a. Drought-wildfire, b.
281 Heat-wildfire, c. Drought-heat, d. Drought-wildfire-heat).

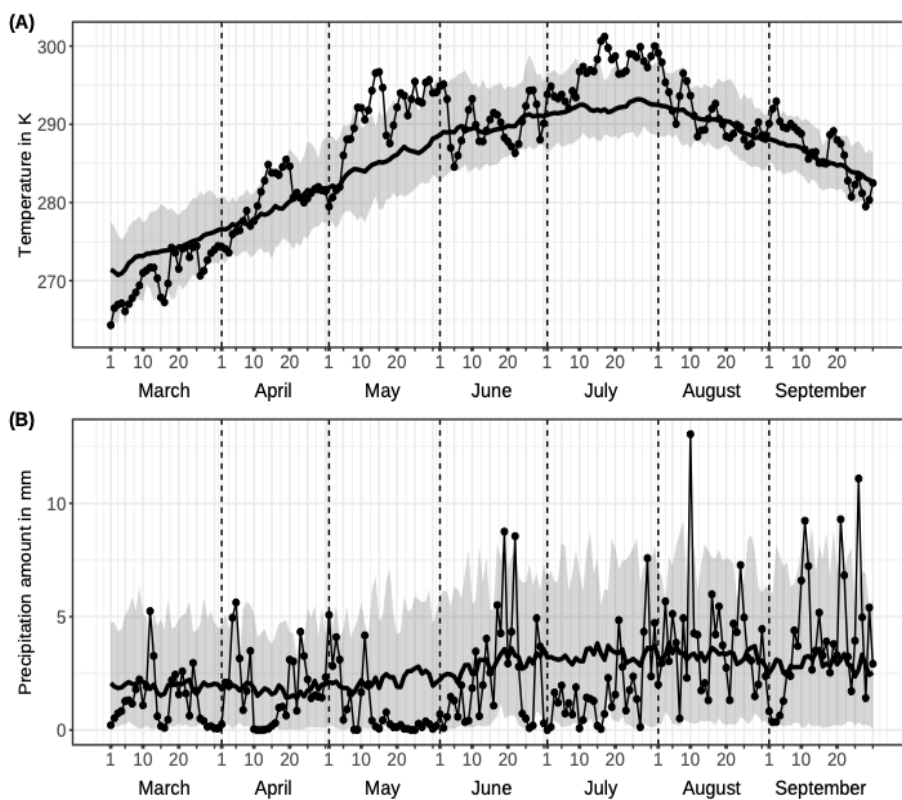
282 3.3 Economic impact of multi-hazard on different sectors – the example of 2018

283 3.3.1 Definition of the compound event of 2018 from a Northern European perspective

284 Figure 7 panel (A) shows the ERA5 maximum temperature values, averaged over the region of Finland, Norway and
285 Sweden, for March to September. The thick black line is the daily climatological mean over 1979-2023 and the gray
286 shaded area the central 90% interval over the same period. The thin black line represents daily values for 2018. Figure
287 7 panel (B) shows the equivalent for daily total precipitation. Overall, temperatures in spring and summer indicate
288 several periods of higher-than-average temperature, which in April and May coincide with periods of low
289 precipitation.

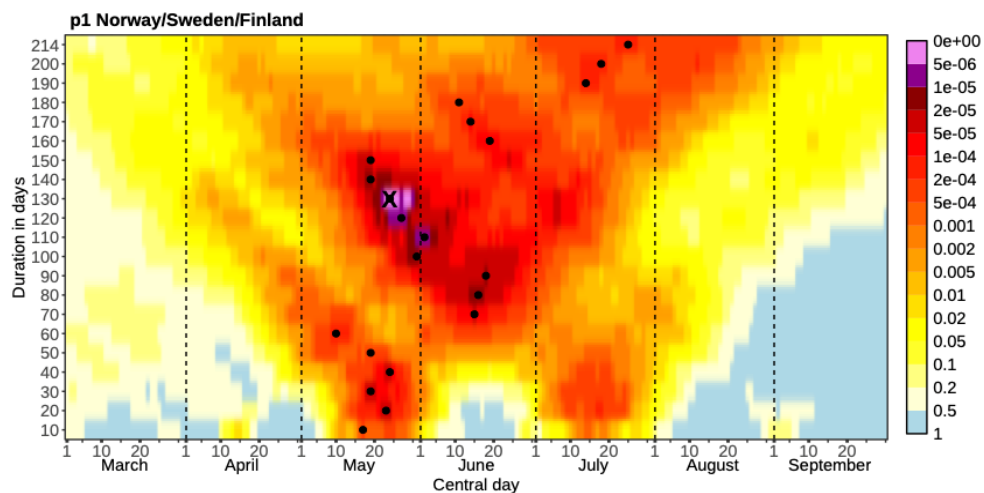
290 As described in Section 2.1, we establish an objective temporal scale for the 2018 combined heatwave and
291 drought by finding the scale with the smallest occurrence probability. These probabilities for all potential scales,
292 ranging from very short (10 days) to the full period between May and September (214 days), are shown in Fig. 8. The
293 central day of the respective time period is shown on the x-axis, with the event duration on the y-axis. The dots mark
294 the scale with the smallest probability for each duration and the X symbol the smallest probability across all scales.
295 Our results show that the 2018 compound heatwave and drought in Norway, Sweden and Finland occurred between
296 22 March and 29 July and lasted for 130 days, thus including most of the hot and dry periods seen in Fig. 7.

297



298

299 **Figure 7. Maximum temperature and precipitation**



300

301 **Figure 8. Smallest probability for an event between 22 March and 29 July 2018.**

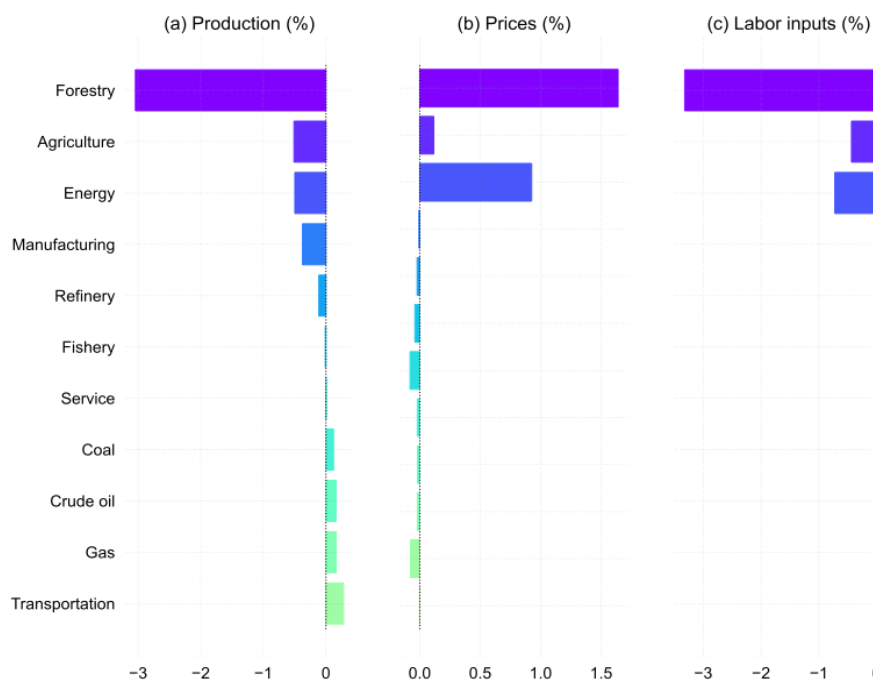


302 **3.3.2 Economic impacts on the local economy**

303 To understand the economic impacts of multiple hazards at the 2018 level, we solve the GRACE model by
 304 incorporating the impact within the model, especially in the energy, agriculture, and forestry sectors of Scandinavian
 305 countries for the year 2018, using estimates as shown in Table 2. The outcomes of sectoral production, prices, trade
 306 patterns and GDP are then compared to the “business-as-usual” (BAU) case, where no hazard events occurred. The
 307 results illustrate both the direct and indirect impact of 2018 compound events on the economy in a cross-sectoral and
 308 cross-regional context. The impacts are evaluated for 33 European countries, other developed countries and the rest
 309 of the world. The results presented in these subsections aggregate the impacts in Norway, Sweden and Finland.

310 In the Scandinavian region, the 2018 compound events contributed to an overall 0.08% drop in GDP
 311 compared to the counterfactual scenario of BAU. It accounts for 2.23 billion NOK in 2018 value computed using 2018
 312 GDP data collected from SSB (2024). Although this decline in GDP was moderate, it was significant enough to draw
 313 attention and had broad impacts on the local economy.

314 Figure 9 depicts the changes in output by sector. Our findings reveal that the production in agriculture,
 315 forestry, and electricity sectors all experienced negative impacts due to the direct effects of multi-hazards. Among
 316 these sectors, the forestry sector suffered the most significant loss of 3.04%. The production of electricity decreased
 317 by 0.50% relative to the business-as-usual case, and the agriculture sector experienced a 0.51% reduction. Meanwhile,
 318 the lowered output in these directly impacted sectors led to an increase in the prices of the products (Fig. 10). Notably,
 319 the domestic price of forestry goods increased by 1.64%, electricity price increased by 0.93%, and the prices of
 320 agricultural goods rose by 0.12%.



321

322 **Figure 9. Direct impacts on the domestic economy by sectors due to 2018 multi-events in Scandinavia**

323

324 The agriculture, forestry and electricity sectors are linked with other parts of the economy through their roles as
 325 intermediate inputs. Consequently, the reduction of production in specific sectors can trigger multiplier effects. This



326 will result in cross-sectoral impacts beyond the initially affected sectors. Figure 9 also demonstrates the significant
327 indirect impact of 2018 compound events on other sectors of the economy in the region. For instance, in panel (a) the
328 production of manufacturing goods had a -0.37% decline caused by the 2018 multi-hazard. It also shows that
329 compound events in 2018 caused a considerable indirect impact on the refined oil sector, with production dropping
330 by nearly -0.11% due to disturbances in energy inputs in the production process. Simultaneously, the substitution
331 effect resulted in an increased demand for crude oil and natural gas, boosting production in those sectors: a 0.16%
332 increase in crude oil production and a 0.17% increase in natural gas production. Furthermore, in panel (b), the domestic
333 price of fossil fuel energy moderately decreased in equilibrium due to these effects (as shown in Fig. 9). Because of
334 the effect on prices, the Scandinavian region would gain a comparative advantage in producing fossil fuels and
335 exporting supplies. This potentially led to a carbon leakage in the region.

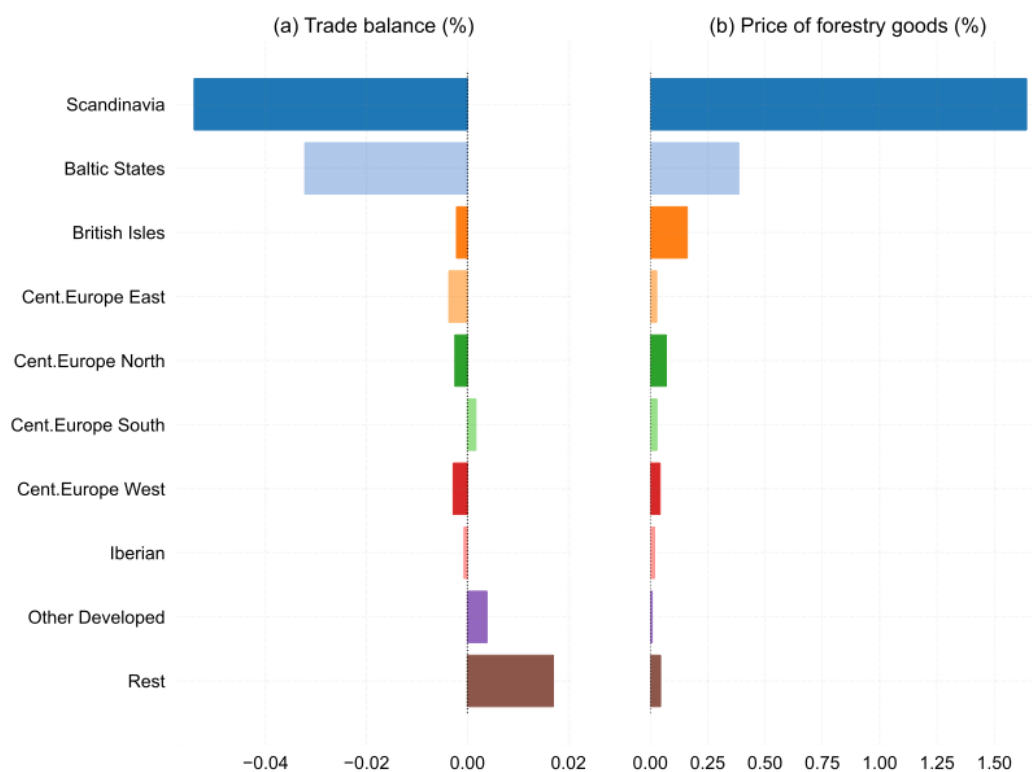
336 Additionally, the decreased production in sectors directly affected by climate change in the Scandinavia
337 region has led to a reduction in labor demand. Consequently, there has been a decrease in labor allocated to these
338 sectors. As shown in Fig. 9 panel (c), labor input in the forestry sector declined by 3.32%, in the agricultural sector by
339 0.44%, and in the electricity sector by 0.72%. However, there has been an observed increase in labor input in other
340 sectors indirectly affected. While this allows for some mobility of labor within the region, the transfer of workers from
341 negatively impacted sectors to others does not completely compensate for the overall decrease in labor demand based
342 on the limitations of labor mobility. Thus, the lower labor inputs potentially lead to an increase in unemployment
343 within the Scandinavia region.

344 **3.3.3 Economic impacts in other regions**

345 The 2018 multi-hazard had a widespread ripple effect on the global economy, especially within Europe². This is
346 particularly due to its significant impact on forestry goods production in the Scandinavian regions. The Scandinavian
347 region has an important role in exporting forestry products. Thus, the 2018 events resulted in a 29.39% reduction in
348 the export of forestry goods, contributing to a 0.05% drop in the trade balance, as indicated in Fig. 10a. Meanwhile,
349 we found that five out of eight European regions, including the British Islands, Central Europe-East, Central Europe-
350 North, Central Europe-West, and the Iberian countries, experienced a decline in their trade balance. These regions are
351 important trading partners of Scandinavian forestry products which highlights the widespread economic impact of
352 2018 multi-hazards across Europe.

353 Despite having a strong forestry sector, the Baltic region is projected to see a 0.03% decrease in its trade
354 balance. This decline is largely due to the dominant position of Scandinavian forestry products in the global market.
355 The reduced supply of forestry goods from Scandinavia could not fulfill the global demand and increased prices of
356 wood products worldwide. As illustrated in Fig. 10 panel (b), wood products from the Baltic states have experienced
357 a 0.39% price increase, the second highest price increase after the Scandinavian region. The large surge in prices
358 created a comparative disadvantage for Baltic forestry products in the global trade market, making them less
359 competitive compared to alternatives. Consequently, this explains the negative ripple effect on the trade balance
360 volume in the Baltic states.

² The results on the country level impacts are aggregated into 8 sub-regions within Europe. Scandinavia includes Norway, Sweden and Finland. Baltic States include Estonia, Latvia, Lithuania. The British Isles include Ireland and the United Kingdom. Eastern Central Europe includes Denmark, Germany, Netherlands, Belgium and Luxembourg. Eastern Central Europe includes the Czech Republic, Hungary, Poland, Slovakia, Slovenia, Albania, Bulgaria, Belarus, Croatia, Romania, and Ukraine. Iberian Peninsula includes Spain and Portugal. Southern Central Europe includes Cyprus, Greece, and Italy. Western Central Europe includes Malta, Austria, and France.



361

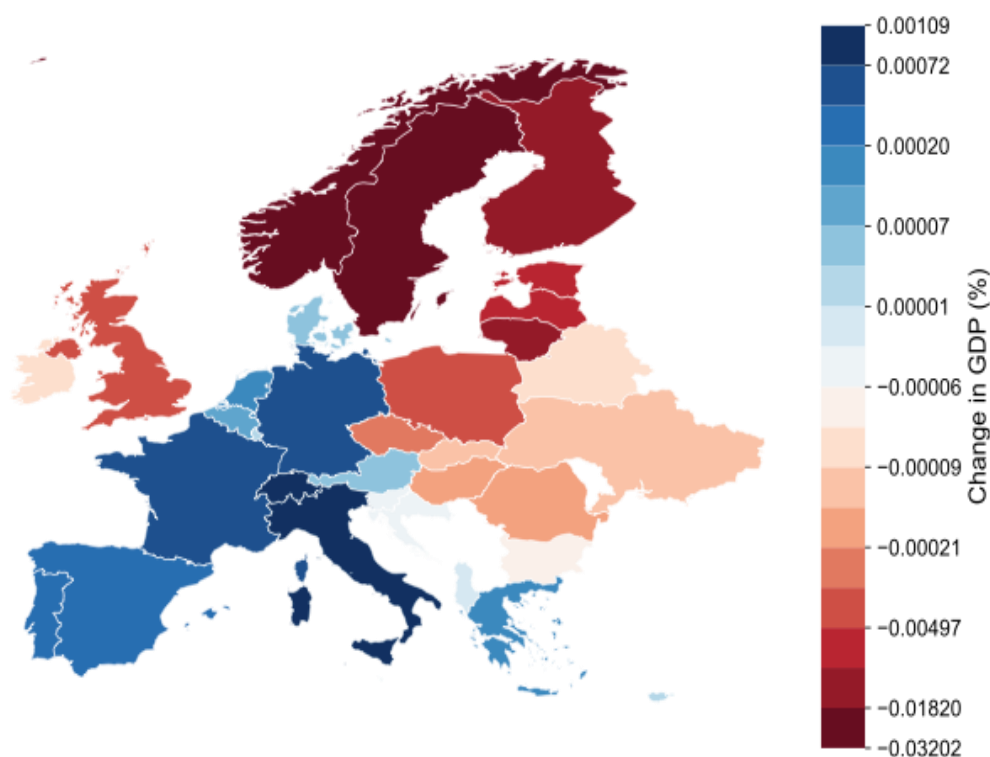
362 **Figure 10.** Abroad economic impacts due to 2018 multi-events

363 Interestingly, our findings indicate that the 2018 disturbances in Scandinavia have stimulated the export of forestry
364 products from other developed countries and the various regions in the rest of the world. These areas have experienced
365 more moderate price increases (as shown in Fig. 10 panel (b)), leading to an implied comparative advantage. It
366 motivated production and export from these remote countries to meet the global demand for forestry products.
367 According to FAOSTAT (2024), the major exporters of forestry products aside from European countries, include
368 developed countries such as the United States, Canada and Russia. The list also extends to other countries, including
369 China and Brazil, among others. These countries also increased their market presence in the forestry sector and thus
370 compensated for the reduced supply from the Scandinavian region.

371 Ultimately, the market effects and trade effects transform the direct, sector-specific impacts into broader
372 cross-sectoral and cross-regional impacts. These cumulative effects contribute to the impact on the GDP of each
373 region. Figure 11 presents the isolated impact on GDP due to the 2018 events in 33 European countries. As shown in
374 Fig. 11, countries in the Baltic states, British Isles, and Central Europe-East have experienced GDP losses caused by
375 2018 compound events, mainly driven by inter-regional trade effects. In contrast, countries in Northern Central
376 Europe, Southern Central Europe, and the Iberian regions have seen GDP growth during the period. The GDP growth
377 in these regions is the result of the combined effects of changes in internal markets or trade patterns. Particularly, Fig.
378 10 shows that Southern Central Europe benefited from the remote impact in the Scandinavia region with an increase
379 in the trade balance due to rising prices of forestry goods, leading to a positive GDP growth as shown in Fig.11.



380



381

382 **Figure 11.** Economic impacts of 2018 compound events: GDP impacts in 33 European countries

383

384 **4 Discussion**

385 This study aims to better understand the impacts and occurrences of multi-hazard events in summer (such as
386 compounding heatwave, drought and wildfire) in Scandinavia from a multidisciplinary perspective. High risk drought-
387 wildfire events occur twice as often as heat-wildfire, and heat-drought events, with spatial patterns ranging primarily
388 along the Norwegian coast, which is in accord with the results from Sutanto et al. (2020). Combinations of wildfire-
389 hazard events primarily occur in Norway, with fewer occurrences in Finland, where several factors such as natural
390 fire breaks and an extensive road network help maintain the fires small and at a low-intensity (Fernandez-Anez et al.,
391 2021). Forest management in Finland is as such that a large majority of the biomass is removed during harvesting,
392 decreasing the amount of available fuel (Fernandez-Anez et al., 2021), although it has been noted that an increase in
393 prescribed burning would be beneficial in order to increase forest biodiversity in the country (Lindberg et al., 2020).

394 Drought-hazard events in Sweden appear to occur in the southern and central regions, where Teutschbein et
395 al. (2022) found that southern catchments experienced more severe streamflow droughts than northern ones.
396 Teutschbein et al. (2022) identified a wetting trend in Sweden during the winter months, with a minor drying trend
397 during the spring and summer, which suggests that drought management measures should be put into place at a
398 regional scale, where regional differences in climate might occur. Blauhut et al. (2022) also mention the urgency of
399 an European drought governance approach in the form of a general framework permitting flexible regional
400 management strategies.



401 All multi-hazard combinations affect significantly moors and heathlands, mainly located along the northern
402 Norwegian-Swedish border and south-western region of Norway (Fig. 5). Dead heather specimens in low humidity
403 air were found by Log et al. (2017) to dry at a surprisingly fast rate, showing they were prone to fire “within two days
404 during wintertime and well within one day in warm weather”. During the winter of 2014, after a 3-week period with
405 no precipitation registered by the Norwegian Meteorological Institute and relatively windy weather, wildfires burned
406 in 2014 a total 35 km² surface area of heathlands (Log et al., 2017). Prescribed burnings had not been performed in
407 the area over the last 50 years, and resulted in an accumulation of dead heather and thus vegetation susceptible to
408 drying and wildfires (Log et al., 2017). Unmanaged heathlands thus pose a fire risk in dry and windy weather, and
409 would benefit from mitigation management measures, especially with fire and drought frequency expected to increase
410 in boreal ecosystems.

411 The main land cover types at risk of heat-related multi-hazards in Scandinavia are vegetated (broad-leaved
412 forests, coniferous forest, sparsely vegetated areas). In multi-hazard hotspots, namely along the northern Norwegian-
413 Swedish border, south-western region of Norway, central Sweden and in the south-eastern region of Finland, forest
414 management mitigation measures could be implemented to decrease this risk. Certain zones at high risk of multi-
415 hazards have actually seen an expansion of a specific land cover (for example Norwegian broad-leaved forests). These
416 regions would benefit from implementing suitable adaptation measures, to decrease the vulnerability of such areas.
417 Not anticipating possible hazards could result in economic losses if a hazard does occur, for example California’s
418 timber production was severely affected by a forest die-off event attributed to the 2012-2015 drought (Sleeter et al.,
419 2018). As Sweden’s and Finland’s economies rely on wood products production and export, it is important to ensure
420 forested areas are adapted to droughts, wildfires and heat waves, particularly when anthropogenic climate change is
421 predicted to intensify fire and drought frequency in boreal ecosystems (Girardin et al., 2010; IPCC, 2021). Especially,
422 our economic assessment of the impact of 2018 multi-hazards reveals a varying and wide-spreading result across
423 sectors and regions, particularly in Europe. Consistent with Beillouin et al. (2020), Bakke et al. (2020) and Gustafsson
424 et al. (2019), our results include reduced agriculture, energy and forestry output in the Scandinavian region as the
425 direct impacts. The sectoral-specific impacts also transfer to other sectors in the Scandinavian economy. For example,
426 we find a decrease in manufacturing production caused by reduced intermediate inputs of agriculture, energy and
427 forestry goods. At the same time, we also find an increase in the production of oil and gas due to the substitution effect
428 of less electricity production. Furthermore, the compound event of 2018 also affected the trade of forestry goods
429 because of the vital role of Scandinavia in the international wood market. This led to a moderate yet widespread effect
430 on GDP losses, affecting not only the Scandinavian region but also trading patterns, particularly in Europe. Sparsely
431 vegetated areas could also benefit from monitoring drought or fire risk in the area. Human activity is responsible for
432 more than 80% of wildfires in Europe, with data suggesting that about 60% of fires are started deliberately (EEA,
433 2020), and human-induced fires spread faster than lightning-induced fires (Hanston et al., 2020). Awareness
434 campaigns to reduce the risk of ignition in areas where vegetation is vulnerable to drought or fire could be carried out
435 by regional governments. Bare rocks are at such a high risk of heat-related multi-hazards due to Sutanto et al.’s (2020)
436 calculations being based on atmospheric data and soil moisture. Bare rocks have low moisture content compared to
437 vegetation, which could explain that they cross the soil moisture drought threshold when only looking at soil moisture.

438 **Limitations and outlook**

439 This study has potential limitations for risk mapping, evaluating impacts, among others. The multi-hazard risk maps
440 were put together using atmospheric data originally used for a heatwave, drought and wildfire risk analysis of
441 continental Europe, which resulted in coarser resolution when cropping to the Scandinavian region. The aim of this
442 study was not to generate new data but to use this previous research to produce multi-hazard risk maps of the selected
443 regions. Due to the scope of this study, the land cover datasets were retrieved from Copernicus’ Land Monitoring
444 Service instead of national land cover datasets. This helped keep the land cover analysis consistent for all three
445 countries included in the study, but also rendered a coarse land cover map of Scandinavia.

446 When assessing the economic impacts of 2018 multi-hazard, our approach also faces certain limitations. First,
447 there is a lack of robust models capable of evaluating the physical impact of multi-hazards on energy and agriculture



448 production. In this research, we employ historical data to estimate the direct impacts of climate change -relevant multi-
449 hazards. Employing past events as a reference point for extreme scenarios could potentially lead to underestimations.
450 Second, our current assessment does not include climate change impacts in regions outside the primary area of study,
451 which may have a significant effect on the socioeconomic impact in the Scandinavia country. This highlights the need
452 for more comprehensive data collection and modeling to assess the direct and indirect impact of multi-hazards in a
453 broader scope.

454 Three main extensions of this study could be potentially considered. Firstly, since drought risk was calculated
455 by Sutanto et al. (2020) by looking at soil moisture data, which specifies soil moisture drought, this study could also
456 be expanded to consider another type of drought (such as hydrological or meteorological drought) when calculating
457 drought risk. Blauhut et al. (2022) recommend, to improve drought risk management, to look at different types of
458 drought, which use different indicators and impact different sectors. For example, a study done by Asner et al. (2015)
459 assessed the 2012-2015 drought in California by looking at forest canopy loss, which displayed a broader range of
460 drought-affected forests than was seen with visual mapping approaches. Secondly, multi-hazard risk maps were
461 generated using past atmospheric data, from 2000 to 2018; an extension of this study could be made by building multi-
462 hazard risk maps on future climate scenarios. Various studies have looked at future drought risk in Europe, such as
463 research conducted by Roudier et al. (2015) and Spinoni et al. (2017), which could provide geospatial data to map
464 future drought risk. Third, we suggest a close investigation into how the stock and productivity of forestry were
465 affected by the 2018 multi-hazards using land surface models, for example, Community Land Model (CLM)
466 (Lawrence et al., 2019). The approach would provide a more accurate assessment of the losses in the forestry sector
467 and also help to refine its spill-over effect on the broader economy. We also recommend extending similar sectoral-
468 specific models for agriculture and energy sectors to capture the full scope of 2018 multi-hazard impacts.

469 Forest management and adaptation measures are crucial to reducing the risk of heat-related multi-hazards in
470 vulnerable vegetated areas of Scandinavia, particularly in multi-hazard hotspots like the Norwegian-Swedish border,
471 as droughts and wildfires, intensified by climate change, could severely impact timber production and regional
472 economies reliant on wood exports. The findings of this study can provide guidance for policy makers regarding forest
473 management in Scandinavia in the current context of anthropogenic climate change. By highlighting the
474 interconnectedness of heat-related events, we aim to emphasize the importance of anticipating these hazards,
475 particularly droughts and wildfires, ultimately mitigating their impacts on the environment and the economy.
476

477 **5 Conclusions**

478 To better understand the interplay of multi-hazard risk of heatwaves, droughts and wildfires in a multi-sectoral context
479 and to improve disaster risk management in a multi-hazard setting, we assess the occurrence of these hazards using a
480 spatial analysis of compound heatwave, droughts and wildfires events from 2000 to 2018 in Scandinavia. Our results
481 show that high risk drought-wildfire events occur twice as often as heat-wildfire, and heat-drought events, with
482 occurrences up to 166 days of the summer seasons between 2000-2018. Furthermore, our analysis suggests that
483 hotspots for compound drought, heat, and wildfire events in Scandinavia are primarily concentrated along the
484 Norwegian coast and the northern Norwegian-Swedish border, with significant overlap in areas prone to all multi-
485 hazard combinations, while inland regions are generally not at risk. When looking at the economic impacts of the
486 2018 compound multi-hazard events, an 0.08% GDP drop in Scandinavia was observed, primarily impacting the
487 forestry sector, which saw a 3.04% decline, alongside cross-sectoral effects and increased prices in agriculture,
488 forestry, and electricity. Furthermore, the same event led to a 29.39% reduction in Scandinavian forestry exports,
489 causing a ripple effect across Europe, with trade balance declines in five European regions and a 0.05% overall drop
490 in the trade balance due to the disruption in the global supply of forestry products. Effective forest management and
491 adaptation are key to reducing the risk of heat-related multi-hazards in vulnerable Scandinavian regions, especially
492 along the Norwegian-Swedish border, where droughts and wildfires, exacerbated by climate change, threaten timber
493 production and regional economies. This study offers guidance for policymakers on mitigating these interconnected
494 hazards to protect both the environment and the economy.



495 *Data availability.* ERA5 reanalysis data is openly available from the Copernicus Climate Change Service (C3S)
496 Climate Data Store (CDS) at <https://cds.climate.copernicus.eu/datasets/reanalysis-era5-single-levels>.
497 CORINE Land Cover data (CLC) is openly available from the Copernicus Land Monitoring Service at
498 <https://land.copernicus.eu/en/products/corine-land-cover>.

499

500 *Author contributions.*

501 Author contributions follow the CRediT authorship categories.

502

503 **Gwendoline Ducros:** Conceptualization, Writing - Original Draft, Data Curation. **Timothy Tiggeloven:**
504 Conceptualization, Writing - Review & Editing, Supervision. **Lin Ma:** Software, Writing - Original Draft, Data
505 Curation. **Anne Sophie Daloz:** Conceptualization, Writing - Review & Editing. **Nina Schuhen:** Investigation,
506 Software, Writing - Original Draft. **Marleende Ruiter:** Conceptualization, Writing - Review & Editing, Supervision.

507

508 *Competing interests.* The contact author has declared that none of the authors has any competing interests

509

510 *Acknowledgements.*

511 T.T., A.S.D., L.M., and M.d.R. were supported by the European Union's Horizon 2020 funded project MYRIAD-EU
512 (Grant 101003276). MCR also received support from the Netherlands Organisation for Scientific Research (NWO)
513 (VENI; grant no. VI.Veni.222.169). Furthermore, this study was partially supported by the ACROBEAR project, a
514 project under the Belmont Forum Collaborative Research Action on Climate, Environment and Health.

515

516 **References**

517 AghaKouchak, A., Chiang, F., Huning, L. S., Love, C. A., Mallakpour, I., Mazdiyasi, O.,
518 Moftakhari, H., Papalexioi, S. M., Ragno, E., & Sadegh, M. (2020). Climate extremes and compound hazards
519 in a warming world. *Annual Review of Earth and Planetary Sciences*, 48(1), 519–548.
520 <https://doi.org/10.1146/annurev-earth-071719-055228>

521 Asner, G. P., Brodrick, P. G., Anderson, C. B., Vaughn, N., Knapp, D. E., & Martin, R. E. (2015).
522 Progressive forest canopy water loss during the 2012–2015 California drought. *Proceedings of the National*
523 *Academy of Sciences*, 113(2). <https://doi.org/10.1073/pnas.1523397113>

524 Åström, C., Bjelkmar, P., Forsberg, B.. (2019). Attributing summer mortality to heat during 2018
525 heatwave in Sweden. *Environmental Epidemiology*, 3, 16–17.
526 <https://doi.org/10.1097/01.ee9.0000605788.56297.b5>

527 Bakke, S. J., Ionita, M., & Tallaksen, L. M. (2020). The 2018 northern European hydrological
528 drought and its drivers in a historical perspective. *Hydrology and Earth System Sciences*, 24(11), 5621–5653.
529 <https://doi.org/10.5194/hess-24-5621-2020>



- 530 Beillouin, D., Schauburger, B., Bastos, A., Ciais, P., & Makowski, D. (2020). Impact of extreme
531 weather conditions on European crop production in 2018. *Philosophical Transactions of the Royal Society B*
532 *Biological Sciences*, 375(1810), 20190510. <https://doi.org/10.1098/rstb.2019.0510>
- 533 Berrang-Ford, L., Siders, A. R., Lesnikowski, A., Fischer, A. P., Callaghan, M. W., Haddaway, N.
534 R., Mach, K. J., Araos, M., Shah, M. a. R., Wannewitz, M., Doshi, D., Leiter, T., Matavel, C., Musah-Surugu,
535 J. I., Wong-Parodi, G., Antwi-Agyei, P., Ajibade, I., Chauhan, N., Kakenmaster, W., . . . Gilmore, E. A.
536 (2021). A systematic global stocktake of evidence on human adaptation to climate change. *Nature Climate*
537 *Change*, 11(11), 989–1000. <https://doi.org/10.1038/s41558-021-01170-y>
- 538 Blauhut, V., Stoelzle, M., Ahopelto, L., Brunner, M. I., Teutschbein, C., Wendt, D. E., Akstinis, V.,
539 Bakke, S. J., Barker, L. J., Bartošová, L., Briede, A., Cammalleri, C., Kalin, K. C., De Stefano, L., Fendeková,
540 M., Finger, D. C., Huysmans, M., Ivanov, M., Jaagus, J., . . . Živković, N. (2022). Lessons from the 2018–
541 2019 European droughts: a collective need for unifying drought risk management. *Natural Hazards and*
542 *Earth System Sciences*, 22(6), 2201–2217. <https://doi.org/10.5194/nhess-22-2201-2022>
- 543 Buras, A., Rammig, A., & Zang, C. S. (2020). Quantifying impacts of the 2018 drought on European
544 ecosystems in comparison to 2003. *Biogeosciences*, 17(6), 1655–1672. [https://doi.org/10.5194/bg-17-1655-](https://doi.org/10.5194/bg-17-1655-2020)
545 2020
- 546 Cattiaux, J., & Ribes, A. (2018). Defining single extreme weather events in a climate perspective.
547 *Bulletin of the American Meteorological Society*, 99(8), 1557–1568. [https://doi.org/10.1175/bams-d-17-](https://doi.org/10.1175/bams-d-17-0281.1)
548 0281.1
- 549 Christensen, O. B., Kjellström, E., Dieterich, C., Gröger, M., & Meier, H. E. M. (2022).
550 Atmospheric regional climate projections for the Baltic Sea region until 2100. *Earth System Dynamics*, 13(1),
551 133–157. <https://doi.org/10.5194/esd-13-133-2022>
- 552 Couasnon, A., Eilander, D., Muis, S., Veldkamp, T. I. E., Haigh, I. D., Wahl, T., Winsemius, H. C.,
553 & Ward, P. J. (2020). Measuring compound flood potential from river discharge and storm surge extremes
554 at the global scale. *Natural Hazards and Earth System Sciences*, 20(2), 489–504.
555 <https://doi.org/10.5194/nhess-20-489-2020>



556 de Ruiter, M. C., Couasnon, A., Van Den Homberg, M. J. C., Daniell, J. E., Gill, J. C., & Ward, P.
557 J. (2020). Why we can no longer ignore consecutive disasters. *Earth's Future*, 8(3).
558 <https://doi.org/10.1029/2019ef001425>

559 de Ruiter, M. C., de Bruijn, J. A., Enghardt, J., Daniell, J. E., de Moel, H., & Ward, P. J. (2021). The
560 synergies of structural disaster risk reduction measures: Comparing Floods and earthquakes. *Earth's Future*,
561 9, e2020EF001531. <https://doi.org/10.1029/2020EF001531>

562 European Commission: Joint Research Centre, Cammalleri, C., Naumann, G., Mentaschi, L.,
563 Formetta, G., Forzieri, G., Gosling, S., Bisselink, B., De Roo, A., & Feyen, L. (2020). Global warming and
564 drought impacts in the EU : JRC PESETA IV project : Task 7, Publications Office.
565 <https://data.europa.eu/doi/10.2760/597045>

566 FAOSTAT (2024) , Forestry Production and Trade, <https://www.fao.org/faostat/en/#data/FO>

567 Fernandez-Anez, N., Krasovskiy, A., Müller, M., Vacik, H., Baetens, J., Hukić, E., Solomun, M.
568 K., Atanassova, I., Glushkova, M., Bogunović, I., Fajković, H., Djuma, H., Boustras, G., Adámek, M.,
569 Devetter, M., Hrabalíková, M., Huska, D., Barroso, P. M., Vaverková, M. D., . . . Cerda, A. (2021). Current
570 wildland fire patterns and challenges in Europe: A synthesis of national perspectives. *Air Soil and Water*
571 *Research*, 14, 117862212110281. <https://doi.org/10.1177/11786221211028185>

572 Girardin, M. P., Ali, A. A., & Hély, C. (2010). Wildfires in boreal ecosystems: past, present and
573 some emerging trends. *International Journal of Wildland Fire*, 19(8), 991.
574 https://doi.org/10.1071/wfv19n8_fo

575 Gustafsson, L., Berglind, M., Granström, A., Grelle, A., Isacson, G., Kjellander, P., Larsson, S.,
576 Lindh, M., Pettersson, L. B., Strengbom, J., Stridh, B., Sävström, T., Thor, G., Wikars, L., & Mikusiński, G.
577 (2019). Rapid ecological response and intensified knowledge accumulation following a north European
578 mega-fire. *Scandinavian Journal of Forest Research*, 34(4), 234–253.
579 <https://doi.org/10.1080/02827581.2019.1603323>

580 Hantson, S., Andela, N., Goulden, M. L., & Randerson, J. T. (2022). Human-ignited fires result in
581 more extreme fire behavior and ecosystem impacts. *Nature Communications*, 13(1).
582 <https://doi.org/10.1038/s41467-022-30030-2>



583 Hersbach, H., Bell, B., Berrisford, P., Biavati, G., Horanýi, A., Muñoz Sabater, J., Nicolas, J.,
584 Peubey, C., Radu, R., Rozum, I., Schepers, D., Simmons, A., Soci, C., Dee, D., Thépaut, J.-N. (2023): ERA5
585 hourly data on single levels from 1940 to present. Copernicus Climate Change Service (C3S) Climate Data
586 Store (CDS). <https://doi.org/10.24381/cds.adbb2d47>

587 IPCC, 2012: Summary for Policymakers. In: *Managing the Risks of Extreme Events and Disasters*
588 to Advance Climate Change Adaptation [Field, C.B., V. Barros, T.F. Stocker, D. Qin, D.J. Dokken, K.L. Ebi,
589 M.D. Mastrandrea, K.J. Mach, G.-K. Plattner, S.K. Allen, M. Tignor, and P.M. Midgley (eds.)]. A Special
590 Report of Working Groups I and II of the Intergovernmental Panel on Climate Change. Cambridge University
591 Press, Cambridge, UK, and New York, NY, USA, pp. 1-19.

592 IPCC, 2021: *Climate Change 2021: The Physical Science Basis. Contribution of Working Group I*
593 to the Sixth Assessment Report of the Intergovernmental Panel on Climate Change [Masson-Delmotte, V., P.
594 Zhai, A. Pirani, S.L. Connors, C. Péan, S. Berger, N. Caud, Y. Chen, L. Goldfarb, M.I. Gomis, M. Huang,
595 K. Leitzell, E. Lonnoy, J.B.R. Matthews, T.K. Maycock, T. Waterfield, O. Yelekçi, R. Yu, and B. Zhou
596 (eds.)]. Cambridge University Press, Cambridge, United Kingdom and New York, NY, USA, In press,
597 doi:10.1017/9781009157896

598 Kueh, M., & Lin, C. (2020). The 2018 summer heatwaves over northwestern Europe and its
599 extended-range prediction. *Scientific Reports*, 10(1). <https://doi.org/10.1038/s41598-020-76181-4>

600 Log, T., Thuestad, G., Velle, L. G., Khattri, S. K., & Kleppe, G. (2017). Unmanaged heathland – A
601 fire risk in subzero temperatures? *Fire Safety Journal*, 90, 62–71.
602 <https://doi.org/10.1016/j.firesaf.2017.04.017>

603 Lindberg, H., Punttila, P., & Vanha-Majamaa, I. (2020). The challenge of combining variable
604 retention and prescribed burning in Finland. *Ecological Processes*, 9(1). [https://doi.org/10.1186/s13717-019-](https://doi.org/10.1186/s13717-019-0207-3)
605 0207-3

606 Lund, M. T., Nordling, K., Gjelsvik, A. B., & Samset, B. H. (2023). The influence of variability on
607 fire weather conditions in high latitude regions under present and future global warming. *Environmental*
608 *Research Communications*, 5(6), 065016. <https://doi.org/10.1088/2515-7620/acdfad>.



- 609 Manuel, L., Chiziane, O., Mandhlate, G., Hartley, F., & Tostão, E. (2021). Impact of climate change
610 on the agriculture sector and household welfare in Mozambique: an analysis based on a dynamic computable
611 general equilibrium model. *Climatic Change*, 167(1–2). <https://doi.org/10.1007/s10584-021-03139-4>
- 612 Matano, A., Van Loon, A., de Ruiter, M., Koehler, J., de Moel, H., and Ward, P.: Compound
613 Drought-Flood Events in Fragile Contexts: Examples from the Horn of Africa, EGU General Assembly 2021,
614 online, 19–30 Apr 2021, EGU21-10148, <https://doi.org/10.5194/egusphere-egu21-10148>, 2021
- 615 Mazdiyasi, O., & AghaKouchak, A. (2015). Substantial increase in concurrent droughts and
616 heatwaves in the United States. *Proceedings of the National Academy of Sciences*, 112(37), 11484–11489.
617 <https://doi.org/10.1073/pnas.1422945112>
- 618 Moftakhari, H., Schubert, J. E., AghaKouchak, A., Matthew, R. A., & Sanders, B. F. (2019). Linking
619 statistical and hydrodynamic modeling for compound flood hazard assessment in tidal channels and estuaries.
620 *Advances in Water Resources*, 128, 28–38. <https://doi.org/10.1016/j.advwatres.2019.04.009>
- 621 Ntombela, C., Nyhodo, B., Ngqangweni, S., Phahlane, H. (2017). Economy-wide effects of drought
622 on South African Agriculture: A computable general equilibrium (CGE) analysis. *Journal of Development
623 and Agricultural Economics*, 9(3), 46–56. <https://doi.org/10.5897/jdae2016.0769>
- 624 NVE (2024). Magasinstatistikk. [https://www.nve.no/energi/analyser-og-](https://www.nve.no/energi/analyser-og-statistikk/magasinstatistikk/)
625 [statistikk/magasinstatistikk/](https://www.nve.no/energi/analyser-og-statistikk/magasinstatistikk/)
- 626 Paprotny, D., Kreibich, H., Morales-Nápoles, O., Castellarin, A., Carisi, F., & Schröter, K. (2020).
627 Exposure and vulnerability estimation for modelling flood losses to commercial assets in Europe. *The Science
628 of the Total Environment*, 737, 140011. <https://doi.org/10.1016/j.scitotenv.2020.140011>
- 629 Raymond, C., Horton, R. M., Zscheischler, J., Martius, O., AghaKouchak, A., Balch, J., Bowen, S.
630 G., Camargo, S. J., Hess, J., Kornhuber, K., Oppenheimer, M., Ruane, A. C., Wahl, T., & White, K. (2020).
631 Understanding and managing connected extreme events. *Nature Climate Change*, 10(7), 611–621.
632 <https://doi.org/10.1038/s41558-020-0790-4>
- 633 Roudier, P., Andersson, J. C. M., Donnelly, C., Feyen, L., Greuell, W., & Ludwig, F. (2015).
634 Projections of future floods and hydrological droughts in Europe under a +2°C global warming. *Climatic
635 Change*, 135(2), 341–355. <https://doi.org/10.1007/s10584-015-1570-4>



- 636 Schuhen, N., Iles, C. E., Cattiaux, J., & Sillmann, J. (2024) Defining compound extreme events on
637 objective spatiotemporal scales. *In preparation*.
- 638 Schipper, E. L. F. (2020). Maladaptation: When adaptation to climate change goes very wrong. *One*
639 *Earth*, 3(4), 409–414. <https://doi.org/10.1016/j.oneear.2020.09.014>
- 640 Scolobig, A., Komendantova, N., & Mignan, A. (2017). Mainstreaming Multi-Risk Approaches into
641 Policy. *Geosciences*, 7(4), 129. <https://doi.org/10.3390/geosciences7040129>
- 642 Sleeter, B., Loveland, T. R., Domke, G. M., Herold, N., Wickham, J., & Wood, N. J. (2018). *Chapter*
643 *5 : Land Cover and Land Use Change. Impacts, Risks, and Adaptation in the United States: The Fourth*
644 *National Climate Assessment, Volume II*. <https://doi.org/10.7930/nca4.2018.ch5>
- 645 Solomon, R., Simane, B., & Zaitchik, B. F. (2021). The impact of climate change on agriculture
646 production in Ethiopia: Application of a Dynamic Computable general equilibrium model. *American Journal*
647 *of Climate Change*, 10(01), 32–50. <https://doi.org/10.4236/ajcc.2021.101003>
- 648 Spinoni, J., Vogt, J. V., Naumann, G., Barbosa, P., & Dosio, A. (2017). Will drought events become
649 more frequent and severe in Europe? *International Journal of Climatology*, 38(4), 1718–1736.
650 <https://doi.org/10.1002/joc.5291>
- 651 SSB (2024). National Accounts. [https://www.ssb.no/en/nasjonalregnskap-og-](https://www.ssb.no/en/nasjonalregnskap-og-konjunkturer/nasjonalregnskap/statistikk/nasjonalregnskap)
652 [konjunkturer/nasjonalregnskap/statistikk/nasjonalregnskap](https://www.ssb.no/en/nasjonalregnskap/statistikk/nasjonalregnskap)
- 653 Sutanto, S. J., Vitolo, C., Di Napoli, C., D'Andrea, M., & Van Lanen, H. A. (2020). Heatwaves,
654 droughts, and fires: Exploring compound and cascading dry hazards at the pan-European scale. *Environment*
655 *International*, 134, 105276. <https://doi.org/10.1016/j.envint.2019.105276>
- 656 Teutschbein, C., Montano, B. Q., Todorović, A., & Grabs, T. (2022). Streamflow droughts in
657 Sweden: Spatiotemporal patterns emerging from six decades of observations. *Journal of Hydrology Regional*
658 *Studies*, 42, 101171. <https://doi.org/10.1016/j.ejrh.2022.101171>
- 659 Tilloy, A., Malamud, B. D., Winter, H., & Joly-Laugel, A. (2019). A review of quantification
660 methodologies for multi-hazard interrelationships. *Earth-Science Reviews*, 196, 102881.
661 <https://doi.org/10.1016/j.earscirev.2019.102881>



- 662 Wahl, T., Jain, S., Bender, J., Meyers, S. D., & Luther, M. E. (2015). Increasing risk of compound
663 flooding from storm surge and rainfall for major US cities. *Nature Climate Change*, 5(12), 1093–1097.
664 <https://doi.org/10.1038/nclimate2736>
- 665 Ward, P. J., De Ruiter, M. C., Mård, J., Schröter, K., Van Loon, A., Veldkamp, T., Von Uexkull,
666 N., Wanders, N., AghaKouchak, A., Arnbjerg-Nielsen, K., Capewell, L., Llasat, M. C., Day, R., Dewals, B.,
667 Di Baldassarre, G., Huning, L. S., Kreibich, H., Mazzoleni, M., Savelli, E., . . . Wens, M. (2020). The need
668 to integrate flood and drought disaster risk reduction strategies. *Water Security*, 11, 100070.
669 <https://doi.org/10.1016/j.wasec.2020.100070>
- 670 Wilcke, R. a. I., Kjellström, E., Lin, C., Matei, D., Moberg, A., & Tyrlis, E. (2020). The extremely
671 warm summer of 2018 in Sweden – set in a historical context. *Earth System Dynamics*, 11(4), 1107–1121.
672 <https://doi.org/10.5194/esd-11-1107-2020>
- 673 Zscheischler, J., & Seneviratne, S. I. (2017). Dependence of drivers affects risks associated with
674 compound events. *Science Advances*, 3(6). <https://doi.org/10.1126/sciadv.1700263>
- 675 Zscheischler, J., Westra, S., Van Den Hurk, B. J. J. M., Seneviratne, S. I., Ward, P. J., Pitman, A.,
676 AghaKouchak, A., Bresch, D. N., Leonard, M., Wahl, T., & Zhang, X. (2018). Future climate risk from
677 compound events. *Nature Climate Change*, 8(6), 469–477. <https://doi.org/10.1038/s41558-018-0156-3>